Effect of Electrode Density of States on the Heterogeneous Electron-Transfer Dynamics of Osmium-Containing Monolayers

Robert J. Forster,*,† Paul Loughman,† and Tia E. Keyes‡

Contribution from the National Centre for Sensor Research, School of Chemical Sciences, Dublin City University, Dublin 9, Ireland, and School of Chemistry, Dublin Institute of Technology, Dublin 4, Ireland

Received July 17, 2000. Revised Manuscript Received September 6, 2000

Abstract: Dense monolayers of $[Os(OMe\text{-}bpy)_2(p3p)Cl]^{1+}$, where OMe-bpy is 4,4′-dimethoxy-2,2′-bipyridyl and p3p is 4,4′-trimethylenedipyridine, have been formed by spontaneous adsorption onto clean platinum, mercury, gold, silver, carbon, and copper microelectrodes. These systems have been used to probe the influence of the electrode density of states on the rate of electron transfer across the electrode/monolayer interface. Monolayers on each material exhibit well-defined voltammetry for the $Os^{2+/3+}$ redox reaction where the supporting electrolyte is aqueous 1.0 M $NaClO_4$. The high scan rate (>2000 V s^{-1}) voltammetric response has been modeled using a nonadiabatic electron-transfer model. The standard heterogeneous electron-transfer rate constant, $k°$, depends on the identity of the electrode material, e.g., $k°$ is 6×10^4 and 4×10^3 s^{-1} for platinum and carbon electrodes, respectively. Chronoamperometry, conducted on a microsecond time scale, has been used to probe the potential dependence of the heterogeneous electron-transfer rate constant. These values range from $(4.0 \pm 0.2) \times 10^4$ to $(3.0 \pm 0.3) \times 10^3$ s^{-1} on going from platinum to carbon electrodes. Temperature-resolved chronoamperometry and cyclic voltammetry reveal that the electrochemical activation enthalpy, $\Delta H^{\ddagger}$, and the reaction entropy, $\Delta S_{RC}^{\ddagger}$, are both independent of the electrode material having values of 11.1 ± 0.5 kJ mol^{-1} and 29.6 ± 2.4 J mol^{-1} K^{-1}, respectively. The effect of electrode material on the preexponential factors is discussed in terms of the electrode density of states. These experimental data indicate that the heterogeneous electron-transfer rate for a nonadiabatic process is not simply proportional to the density of states but is modulated by the electronic coupling efficiency. Moreover, the matrix coupling elements, H_{AB}, are between 0.1 and 0.5 J mol^{-1}, which is approximately 4 orders of magnitude smaller than those found from studies of intervalence charge-transfer intensities within comparable dimeric complexes.

Introduction

Processes as diverse as corrosion inhibition, charging and discharging of batteries, electroanalysis, and medical device operation involve electron transfer across an interface consisting of metallic and molecular species.[1] Failure to develop comprehensive theoretical models that describe how the properties of *both* components dictate the overall rates of electron transfer will impede the development of molecule-based electronics.[2] A two-pronged approach to addressing this issue is most likely to lead to success. A powerful mechanistic insight into the factors that influence electron transfer across molecular species has been obtained using ordered monolayers of redox active materials on electrodes. In recent years they have helped revolutionize our understanding of the role that distance, structure, and the redox composition of the monolayer play in dictating the rate and mechanism of electron transfer.[3] However, the effect of changing the nature of the electrode material has not been probed with the same intensity. This situation is surprising given that traditional theory predicts that for electron transfer involving weakly coupled reactants the heterogeneous electron transfer rates should be directly proportional to the density of states, ρ_F, in the electrode.[4] However, a recent theoretical model developed by Marcus and Gosavi[5] predicts that the coupling strength between the redox center and the electrode will make the electron-transfer rate less sensitive to ρ_F. This observation offers an important new approach to controlling the rate of nonadiabatic heterogeneous electron transfer.

Some attempts have been made to test the effect of changing the electrode material on the electron-transfer dynamics.[6,7,8] Although some discrepancies exist, the general conclusion of these investigations was that the rate of heterogeneous electron transfer is independent of the nature of the electrode. However, measurements involving solution phase reactants are highly sensitive to the purity and history of the electrode, to the pretreatment regime, to double layer effects, and to adsorption of the analyte. Moreover, one cannot easily control the strength of electronic coupling between the electrode and the reactant.

* To whom correspondence should be addressed.
† School of Chemical Sciences.
‡ Dublin Institute of Technology.

(1) Bard, A. J.; Abruña, H. D.; Chidsey C. E. D.; Faulkner, L. R.; Feldberg, S. W.; Itaya, K.; Majda, M.; Melroy, O. S.; Murray, R. W.; Porter, M, D.; Soriaga, M. P.; White, H. S. *J. Phys. Chem.* **1993**, *97*, 7147.
(2) Stoddart, J. F. In *Frontiers in Supramolecular Organic Chemistry and Photochemistry*; Schneider, H. J., Dürr, H., Eds.; VCH: Weinheim, Germany, 1990.
(3) Finklea, H. O. In *Encyclopedia of Analytical Chemistry*; Meyers, R. A., Ed.; Wiley: New York, 2000.
(4) Parsons, R. *Surf. Sci.* **1964**, *2*, 418.
(5) Gosavi, S.; Marcus, R. A. *J. Phys. Chem. B* **2000**, *104*, 2067.
(6) Capon, A.; Parsons, R. *J. Electroanal. Chem.* **1973**, *46*, 215.
(7) Iwasita, T.; Schmickler, W.; Schultze, J. *J. Am. Chem. Soc.* **1984**, *106*, 1233.
(8) Van Venrooij, T. G. J.; Sluyters-Rehbach, M.; Sluyters, J. H. *J. Electroanal. Chem.* **1996**, *419*, 61.

10.1021/ja002616u CCC: $19.00
Published on Web 11/11/2000

Chart 1

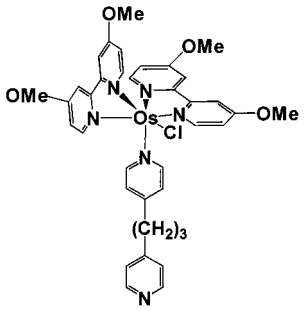

Adsorbed monolayers represent an alternative approach to investigating this issue. They are attractive in that diffusive mass transport is eliminated, double layer effects may be less pronounced, and the reaction can be rendered nonadiabatic simply by controlling the electron-transfer distance or the structure of the bridging ligand. Weaver and co-workers[9] probed the reduction kinetics of adsorbed [$Co^{III}(NH_3)_5$ thiophenecarboxylate] complexes on mercury, gold, and copper electrodes. The heterogeneous electron-transfer rate constants, $k°$, were found to be in the order Hg $\gtrsim$ Au $>$ Cu. However, the rate constants for gold and copper depended on the surface coverage and the effect of bridge conjugation on the adiabaticity of the reaction makes it difficult to extract quantitative information from these experiments. Moreover, these studies did not consider the possibility that the electrode material might influence the free energy of activation.

Here, we have formed spontaneously adsorbed monolayers of $[Os(OMe\text{-}bpy)_2(p3p)Cl]^+$ (Chart 1) on carbon-fiber, mercury, platinum, gold, copper, and silver microelectrodes, where OMe is 4,4′-dimethoxy-2,2′-bipyridyl and p3p is 4,4′-trimethylenedipyridine. This complex has a low redox potential ($\approx$0.05 V) making it possible to probe the electrochemical properties even on rather electropositive metals. The voltammetric response is unusually ideal across a wide range of experimental time scales, temperatures, and electrolyte solutions making it an attractive model system for probing density of states issues. In particular, we are interested in probing how the different orbitals of these metals that contribute to the overall density of states influence the electron-transfer dynamics. For example, the s electrons dominate ρ_F for metals such as gold and silver while the higher density of states for platinum arises predominantly because its d orbitals lie near the Fermi level. The Marcus−Gosavi[5] model predicts that the efficiency with which these different orbitals couple with the localized molecular states of the adsorbate may vary significantly. To address these issues, we have performed detailed measurements of both the potential and temperature dependence of k. These results confirm that the electron transfer is nonadiabatic and that the free energy of activation is dictated by outer-sphere reorganization of solvent dipoles.

Experimental Section

Materials. The surface-active complex $[Os(OMe\text{-}bpy)_2(p3p)Cl]PF_6$ was prepared from $[Os(OMe\text{-}bpy)_2Cl_2]$, which was synthesized as described by Heller and co-workers.[10] A 138 mg (0.2 mmol) amount of $[Os(OMe\text{-}bpy)_2\ Cl_2]$ was placed in 40 cm^3 of methanol and refluxed for 10 min to ensure complete dissolution. A solution of 40 mg (0.2 mmol) of 1,4-trimethylenedipyridine dissolved in 10 cm^3 of methanol was added, and the solution was refluxed for 15 h. The progress of the reaction was monitored using HPLC and cyclic voltammetry. After the reaction was complete, the volume was reduced to 5 cm^3 by rotary evaporation. Ammonium hexafluorophosphate (95+%, Aldrich) was then added, and the dark purple product was collected by filtration and washed with diethyl ether. The product was recrystallized from aqueous methanol to give dark purple-black crystals, yield 160 mg, 82%. Anal. Calcd for $C_{37}H_{38}O_4N_6OsClPF_6$: C, 44.37; H, 3.79; N, 8.39. Found: C, 44.8; H, 3.3; N, 8.2. The complex was further characterized using IR, UV−vis, NMR, and cyclic voltammetry.

Apparatus. Electrochemical cells were of conventional design and were thermostated to within ±0.2 °C using a Julabo F10-HC refrigerated circulating bath. All potentials are quoted with respect to a Ag/AgCl reference electrode. Cyclic voltammetry was performed using a CH Instruments model 660 Electrochemical Workstation and a conventional three-electrode cell. All solutions were degassed using nitrogen, and a blanket of nitrogen was maintained over the solution during all experiments.

In high-speed chronoamperometry,[11] a custom built function generator−potentiostat, with a rise time of less than 10 ns, was used to apply potential steps of variable pulse width and amplitude directly to a two-electrode cell. A Pt foil and an Ag/AgCl reference electrode were combined to form a counter electrode. The foil lowered the resistance and provided a high-frequency path.

Microelectrodes were fabricated from platinum, gold, copper, and silver microwires (Goodfellow Metals Ltd.) as well as carbon fibers of radii between 1 and 25 μm by sealing them under vacuum in soft glass.[12] Where appropriate, the real or microscopic surface area of the electrodes was found by calculating the charge under the oxide or hydrogen adsorption−desorption peaks.[13] Typically, the surface roughness factor was between 1.3 and 1.6. The surface roughness of the carbon microelectrode was estimated as 2.2 on the basis of scanning electron microscopy images.

RC cell time constants, measured in blank electrolyte solution, were between 0.01 and 0.5 μs depending on the electrode material and radius as well as the supporting electrolyte concentration. The interfacial kinetics were measured only at times greater than about 5−10 *RC*. This condition was satisfied by selecting a microelectrode of appropriate radius.

Spontaneously adsorbed monolayers were formed in-situ using a 10 μM solution of the metal complex in the electrolyte solution of interest. Unless otherwise stated, all electrochemical measurements were performed with this concentration of $[Os(OMe\text{-}bpy)_2(p3p)Cl]^+$ in solution. A low concentration of the surface active complex in solution improved the stability of the monolayers yet minimized the diffusional contribution to the overall current in chronoamperometry or cyclic voltammetry. For example, at a 5 μm radius microelectrode the solution phase component contributes less than 5% to the overall Faradaic current for scan rates greater than 5 V s^{-1}.

A nonisothermal cell, where the reference electrode was isolated from the main compartment by a salt bridge and held at room temperature, was used for the temperature-resolved experiments. The nonisothermal salt bridge contained saturated KCl since it has a low resistance, and the salt remains soluble at the lowest temperature employed (−5 °C). The high electrolyte concentration and the design of the bridge minimize any systematic error in the reported temperature effects on $E°'$ due to changes in the liquid junction potential with temperature.[14]

Results and Discussion

General Electrochemical Properties. Figure 1 shows representative cyclic voltammograms obtained at 50 V s^{-1} for $[Os(OMe\text{-}bpy)_2(p3p)Cl]^+$ monolayers spontaneously adsorbed on carbon, gold, mercury, and platinum microelectrodes, where the

(9) Barr, S. W.; Guyer, K. L.; Li, T. T-T.; Liu, H. Y.; Weaver, M. J. *J. Electrochem. Soc.* **1984**, *131*, 1626.

(10) Taylor, C.; Kenaussis, G.; Katakis, I.; Heller, A. *J. Electroanal. Chem.* **1995**, *396*, 511.

(11) Xu, C. Ph.D. Thesis, University of Illinois at Urbana-Champaign, 1992.

(12) Faulkner, L. R.; Walsh, M. R.; Xu, C. *Contemporary Electroanalytical Chemistry*; Plenum Press: New York, 1990.

(13) Trasatti, S.; Petrii, O. A. *J. Electroanal. Chem.* **1992**, *327*, 354.

(14) Yee, E. L.; Cave, R. J.; Guyer, K. L.; Tyma, P. D.; Weaver, M. J. *J. Am. Chem. Soc.* **1979**, *101*, 1131.

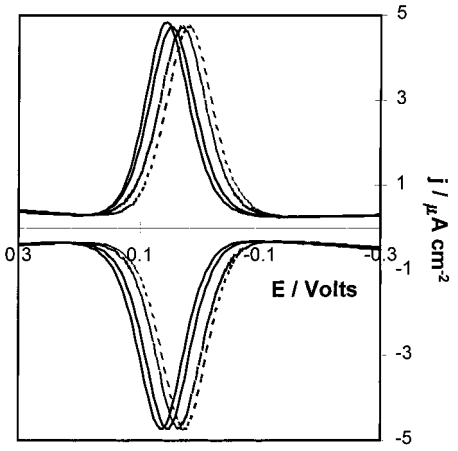

Figure 1. Cyclic voltammograms for the $Os^{2+/3+}$ redox reaction within spontaneously adsorbed $[Os(OMe\text{-}bpy)_2(p3p)Cl]^+$ monolayers. From right to left the electrode material is platinum gold, carbon, and mercury. The scan rate is 50 V s^{-1}, and the surface coverage is $1.0 \pm 0.1 \times 10^{-10}$ mol cm^{-2}. The supporting electrolyte is aqueous 1.0 M $NaClO_4$.

supporting electrolyte is aqueous 1.0 M $NaClO_4$. The formal potentials, $E^{\circ\prime}$, are 0.030, 0.048, 0.060, and 0.120 V for platinum, gold, carbon, and mercury electrodes, respectively. In contrast, the $E^{\circ\prime}$ observed for the complex dissolved in acetonitrile is 0.010 ± 0.008 V irrespective of the electrode material used. The shift in $E^{\circ\prime}$ toward more positive potentials indicates that it is more difficult to oxidize the Os^{2+} redox center when it is adsorbed. Moreover, the differences observed in $E^{\circ\prime}$ suggest that the electron density on the metal center depends on the identity of the electrode material. These differences reflect changes in the free energy of adsorption on the different materials which increase by up to 8.6 kJ mol^{-1} on going from gold to mercury.

Under these slow scan rate conditions, the voltammetric response is consistent in all respects with that expected for an electrochemically reversible reaction involving a surface-confined species.[15] For example, the peak shapes are independent of scan rate, v, at least over the range 1 to 5 V s^{-1}, and the peak height scales linearly with the scan rate unlike the $v^{1/2}$ dependence observed for the complex dissolved in acetonitrile. Consistent with the transfer of a single electron per redox center, the full width at half-maximum is between 100 and 110 mV.[16]

Irrespective of the identity of the electrode material, the surface coverage, Γ, of the redox centers, as determined by integrating the Faradaic charge under the $Os^{2+/3+}$ wave, is $(1.0 \pm 0.1) \times 10^{-10}$ mol cm^{-2}, corresponding to an area occupied per molecule of 168 ± 17 Å^2. The surface coverage does not increase further if the concentration of the surface active complex in solution or the deposition time are increased. This limiting surface is typical of that reported previously by us[17,18] and others for related systems.[19,20] The insensitivity of the saturation coverage to the electrode material indicates that the packing density is controlled by the size of the adsorbate and perhaps lateral interactions rather than by the interatomic spacing of the metal or carbon lattice.

Electron-Transfer Dynamics. Figure 2 illustrates the high-speed voltammetric behavior observed for monolayers immobilized on carbon and platinum microelectrodes. The peak-to-peak separations, ΔE_P, are significantly larger than those observed at long experimental time scales. Uncompensated cell resistance and slow heterogeneous electron transfer could contribute to the observed behavior. Where the working electrode is a 5 μm radius microelectrode, the uncompensated resistance as measured using potential step chronoamperometry is 8125 ± 275 Ω irrespective of whether the electrode is carbon or platinum. Taken in conjunction with the peak maximum peak current observed for the platinum microelectrode, 885 nA, this cell resistance leads to an *iR* drop of approximately 5 mV. This ohmic loss is negligible compared to the peak-to-peak separations of 275 and 60 mV observed for $[Os(OMe\text{-}bpy)_2(p3p)Cl]^+$ monolayers adsorbed on a carbon fiber and platinum microelectrodes, respectively. Therefore, it appears that heterogeneous electron transfer influences the voltammetric response at these high scan rates. Moreover, that ΔE_P is very much larger for monolayers on carbon than on platinum indicates that the standard heterogeneous electron-transfer rate constant, k°, depends on the identity of electrode material.

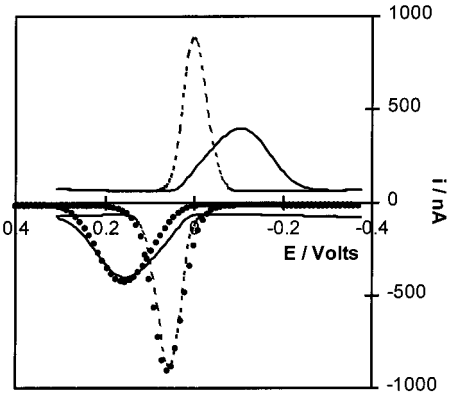

Figure 2. Experimental voltammetric responses for 5 μm radius carbon (—) and platinum (---) microelectrodes modified with $[Os(OMe\text{-}bpy)_2(p3p)Cl]^+$ monolayers. The scan rate is 2000 V s^{-1}, and the supporting electrolyte is 1.0 M aqueous $NaClO_4$. The data points represent optimized fits to a nonadiabatic electron-transfer model in which k° is 4×10^3 and 6×10^4 s^{-1} for carbon and platinum, respectively. The free energy of activation, $\Delta G^\ddagger$, is 6.8 kJ mol^{-1} for both electrode materials.

As discussed elsewhere, k° depends on both a frequency factor and a Franck−Condon barrier and is described by[21−23]

$$k^\circ = A_{et} \exp(-\Delta G^\ddagger/RT) \qquad (1)$$

where A_{et} is the preexponential factor and $\Delta G^\ddagger$ is the electrochemical free energy of activation.[24] For an adiabatic reaction, the prefactor is given by the product of k_{el} the electronic transmission coefficient and v_n a frequency factor dictated either by nuclear or solvent motion. In contrast, for a nonadiabatic reaction $k_{el} \ll 1$ and the prefactor is dictated by the electron hopping frequency in the activated complex, v_{el}.

To understand how differences in the density of states influence electron-transfer dynamics, it is essential to decouple the contributions from electronic coupling effects (A_{et}) and free energies of activation ($\Delta G^\ddagger$).[18,25] This separation may be important for measurements of this kind since distinct film

(15) Laviron, E. *J. Electroanal. Chem.* **1974**, *52*, 395.
(16) Brown, A. P.; Anson, F. C. *Anal. Chem.* **1977**, *49*, 1589.
(17) Forster, R. J.; Faulkner, L. R. *J. Am. Chem. Soc.* **1994**, *116*, 5453.
(18) Forster, R. J.; O'Kelly, J. P. *J. Phys. Chem.* **1996**, *100*, 3695.
(19) Acevedo, D.; Abrûna, H. D. *J. Phys. Chem.* **1991**, *95*, 9590.
(20) Acevedo, D.; Bretz, R. L.; Tirado, J. D.; Abrûna, H. D. *Langmuir* **1994**, *10*, 1300.
(21) Bagchi, G. *Annu. Rev. Chem.* **1989**, *40*, 115.
(22) Sutin, N. *Acc. Chem. Res.* **1982**, *15*, 275.
(23) Li, T. T.-T.; Guyer, K. L.; Barr, S. W.; Weaver, M. J. *J. Electroanal. Chem.* **1984**, *164*, 27.
(24) Sutin, N.; Brunschwig, B. S. *ACS Symp. Ser*. **1982**, *No. 198*, 105.
(25) Forster, R. J.; Vos, J. G. and Keyes, T. E. *Analyst* **1998**, *123*, 1905.

structures may cause the local microenvironment and hence $\Delta G^{\ddagger}$ to depend on the identity of the electrode material.

One approach to decoupling these two contributions is to measure electron-transfer rate constants at a single temperature over a wide range of driving forces. For example, Chidsey,[26] Creager,[27] and Murray[28] have modeled the cyclic voltammograms obtained for long-chain ferrocene alkanethiol according to a nonadiabatic electron-transfer model.

In this model, the anodic rate constant is given by the integral over energy (ϵ) of three functions: (a) the Fermi function for the metal $n(\epsilon)$; (b) a Gaussian distribution of energy levels for acceptor states in the monolayer $D_{Ox}(\epsilon)$; (c) a probability factor describing electron tunneling at a given energy, $P(\epsilon)$.

$$k_{Ox}(\eta) = A\int_{-\infty}^{\infty} D_{Ox}(\epsilon)\, n(\epsilon)\, P(\epsilon)\, d\epsilon \qquad (2)$$

The zero point of energy is defined as the Fermi level of the metal at the particular overpotential of interest. The Fermi function describes the distribution of occupied states within the metal and is defined by

$$n(E) = \left(\frac{1}{1 + \exp[(\epsilon - \epsilon_F)/k_B T]}\right) \qquad (3)$$

where ϵ is the energy of a given state in the electrode, ϵ_F is the Fermi level of the electrode, i.e., the applied overpotential, and k_B is the Boltzmann constant. The density of acceptor states is derived from the Marcus theory[29,30] and is represented by eq 4,

$$D_{Ox}(\epsilon) = \exp\left[-\frac{(\epsilon + \eta - \lambda)^2}{4k\lambda T}\right] \qquad (4)$$

where λ is the reorganization energy ($\equiv 4\Delta G^{\ddagger}$). The distance dependence of electron tunneling[31,32] is given by eq 5, where d

$$P(\epsilon) = \exp(-\beta d) \qquad (5)$$

is the electron-transfer distance. Previous investigations[17] suggest that β is close to 1.6 Å^{-1} for this bridging ligand.

The voltammetric current for the reaction of an immobilized redox center following first-order kinetics is given by[28]

$$i_F = nFA(k_{Ox}(\eta)\Gamma_{Red,\eta} - k_{Red}(\eta)\Gamma_{Ox,\eta}) \qquad (6)$$

where $\Gamma_{Red,\eta}$ and $\Gamma_{Ox,\eta}$ are the instantaneous surface coverages of the oxidized and reduced species and $k_{Ox}(\eta)$ and $k_{Red}(\eta)$ are the reaction rate constants given by eq 2 or its complement in which $n(\epsilon)$ is replaced with $(1- n(\epsilon))$ and $-\lambda$ is replaced by $+\lambda$ in eq 4. Energy minimized molecular modeling indicates that the electron transfer distance, d, is approximately 13.6 Å. Therefore, in using eq 6 to model the voltammetric response, there are only two freely adjustable parameters, $k°$ and $\Delta G^{\ddagger}$ ($=\lambda/4$). To fit the experimental voltammograms, we have used the Nelder and Mead Simplex[33] algorithm to find the values of $k°$ and $\Delta G^{\ddagger}$ that minimize the sum square residuals between the theoretical and experimental currents observed in anodic branches of the linear sweep voltammograms. Figure 2 shows the fits obtained for $[Os(OMe\text{-}bpy)_2(p3p)Cl]^+$ monolayers immobilized on both platinum and carbon fiber microelectrodes. In both cases satisfactory agreement is observed indicating that the electron transfer can be satisfactorily described as a nonadiabatic process. Under these circumstances, one would expect the rate of heterogeneous electron transfer to depend directly on the density of states in the electrode.

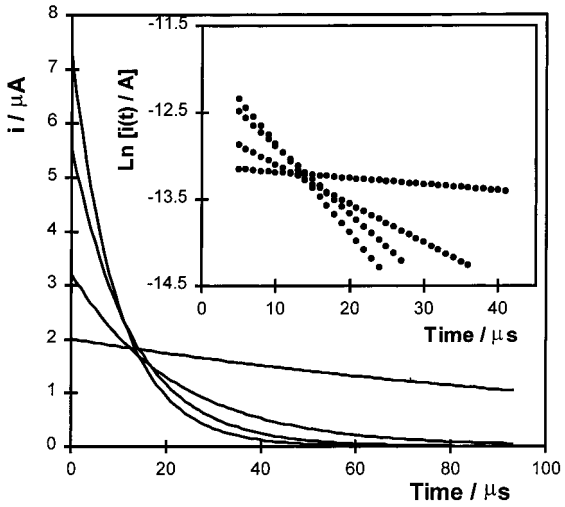

Figure 3. Current response for $[Os(OMe\text{-}bpy)_2(p3p)Cl]^+$ monolayers following a potential step where the overpotential η was 50 mV. From top to bottom on the left-hand side the decays are for platinum, mercury, gold (5 μm), and carbon (12.5 μm). The supporting electrolyte is aqueous 1.0 M $NaClO_4$. The inset shows ln $i_F(t)$ vs t plots for the Faradaic reaction.

The optimized values for $k°$ are 6×10^4 and 4×10^3 s^{-1} for platinum and carbon electrodes, respectively. These values are independent of the scan rate to within 15% for $1000 \le v \le 10\,000$ V s^{-1}. The fit shown in Figure 2 is for a common $\Delta G^{\ddagger}$ of 6.8 kJ mol^{-1}. This analysis suggests that the free energy of activation is independent of the identity of the electrode material and that $k°$ is larger for the platinum electrode because of a larger preexponential factor. However, the quality of the fit shown in Figure 2 is not particularly sensitive to $\Delta G^{\ddagger}$; e.g., increasing $\Delta G^{\ddagger}_{Pt}$ by 25% increases the residual sum of squares between the predicted and experimental peak currents by less than 10%. Therefore, while fitting of the cyclic voltammograms can provide a convenient approach for the determination of $k°$, for this system it appears to provide only an approximate value for $\Delta G^{\ddagger}$. In contrast, temperature-resolved chronoamperometry can be used to accurately probe both the potential dependence of the heterogeneous electron-transfer rate and the free energy of activation.[17,34]

Chronoamperometry. For an ideal electrochemical reaction involving a surface-bound species, the Faradaic current following a potential step that changes the redox composition of the monolayer exhibits a single-exponential decay in time according to[26,35]

$$i_F(t) = kQ\exp(-kt) \qquad (7)$$

where k is the apparent rate constant for the overall reaction and Q is the total charge passed in the redox transformation.

Figure 3 illustrates typical examples of the current−time transients observed for the $Os^{2+} + e^- \rightarrow Os^{3+}$ redox reaction of $[Os(OMe\text{-}bpy)_2(p3p)Cl]^+$ monolayers on different electrode

(26) Chidsey, C. E. D. *Science* **1991**, *251*, 919.
(27) Weber, K.; Creager, S. E. *Anal. Chem.* **1994**, *66*, 3164.
(28) Tender, L.; Carter, M. T.; Murray, R. W. *Anal. Chem.* **1994**, *66*, 3173.
(29) Marcus, R. A. *J. Chem. Phys.* **1956**, *24*, 966.
(30) Marcus, R. A. *J. Phys. Chem.* **1963**, *67*, 853.
(31) Schmickler, W. *J. Electroanal. Chem.* **1977**, *82*, 65.
(32) Bockris, J. O'M.; Khan, S. U. M. *Quantum Electrochemistry*; Plenum Press: New York, 1979; Chapter 8.
(33) Ebert, K.; Ederer, H.; Isenhour, T. L *Computer Applications in Chemistry: An Introduction for PC Users*; VCH Publishers: New York, 1989.
(34) Forster, R. J. *Anal. Chem.* **1996**, *68*, 3143.
(35) Finklea, H. O.; Hanshew, D. D.*J. Am. Chem. Soc.* **1992**, *114*, 3173.

Table 1. Electrode Response Times, Total Cell Resistances, *R*, and Area Normalized Interfacial Capacitances for $[Os(OMe\text{-}bpy)_2(p3p)Cl]^{2+}$ Monolayers Assembled on Various Electrode Materials[a]

electrode	*RC*/ns[b]	*R*/kΩ	C/μF cm^{-2}
platinum	171 ± 30	8.4 ± 0.3	26 ± 4
mercury	135 ± 20	7.8 ± 0.1	22 ± 3
gold	162 ± 26	8.2 ± 0.3	25 ± 3
silver	180 ± 46	8.1 ± 0.4	28 ± 6
carbon	440 ± 90	3.3 ± 0.1	27 ± 5

[a] Measured using potential step chronoamperometry from −0.150 to −0.100 V. The monolayer is in the 1+ oxidation state. The supporting electrolyte is aqueous 1.0 M $NaClO_4$. [b] The electrode radius is 5 μm except for carbon where it is 12.5 μm.

materials. In these experiments the overpotential η ($\equiv E - E^{\circ\prime}$) was 0.05 V. To use these data to accurately measure *k*, the response time of the electrode must be shorter than the time constant for heterogeneous electron transfer. The *RC* time constants for the different electrodes, where *R* is the total cell resistance and *C* is the interfacial capacitance, were obtained by stepping the potential from −0.100 to −0.050 V. The monolayer is not redox active at these potentials, and the current decays follow single-exponential kinetics due to double layer charging. Table 1 contains the resistance, capacitance, and *RC* time constants for each of the electrodes. Table 1 shows that, irrespective of the electrode material, the 5 μm radius electrodes all have response times that are less than 500 ns. This result means that double layer charging will only contribute to the currents observed in Figure 2 only at time scales shorter than approximately 1.5 μs. Therefore, the heterogeneous electron-transfer rate constant can be measured by analyzing the current−time transients at relatively longer time scales. Beyond the issue of convolution between double-layer charging currents and the Faradaic response, Table 1 also confirms that current−time transients of Figure 2 are not compromised by ohmic effects. For example, the total cell resistance for the 10 μm radius silver electrode is approximately 8 kΩ. Therefore, the *iR* drop will be less than 10 mV for times longer than approximately 8 μs. The inset of Figure 2 supports this analysis since, in accordance with eq 7, semilog current vs time plots are linear over at least 1.5 lifetimes. Deviations from linearity would be expected if substantial ohmic drop effects were present. Uncompensated resistance causes the applied potential and, hence, the apparent rate to evolve with time. Therefore, *iR* drop would produce negative deviations in the observed current at short times.[36]

For each electrode material, heterogeneous electron transfer is characterized by a single rate constant indicating that electron transfer is characterized by a single electron-transfer distance, reorganization energy, and microenvironment. Further evidence supporting the predominance of a single rate constant at high concentrations of supporting electrolyte is obtained by examining the intercept of the semilog plot at zero time. As indicated by eq 7, the intercept for a single-exponential decay is ln(*kQ*). We find that the charges passed in chronoamperometry agree with those found in slow scan cyclic voltammetry to within 10%. This agreement indicates that all of the surface confined molecules are redox active on a microsecond time scale.

Figure 4 illustrates Tafel plots of ln *k* vs η for monolayers formed on platinum, gold, and carbon microelectrodes. The dependence of ln *k* on η is clearly nonlinear at large overpotentials, and the slopes decrease in magnitude with increasing overpotential in both anodic and cathodic directions. This

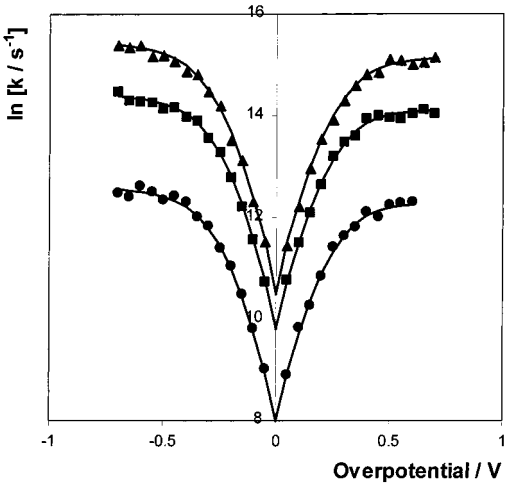

Figure 4. Tafel plot for $[Os(OMe\text{-}bpy)_2(p3p)Cl]^+$ monolayers adsorbed on platinum (▲), gold (■), and carbon (●) microelectrodes. The supporting electrolyte is 1.0 M aqueous $NaClO_4$. The solid curves represent best fits derived from the nonadiabatic electron-transfer model (eqs 2−5). For platinum, gold, and carbon, k° is 4.0×10^4, 1.8×10^4, and 3×10^3 s^{-1}, respectively, while λ is constant at 27 kJ mol^{-1}. Between monolayer error bars are approximately the same size as the symbols.

behavior contrasts with the predictions of the conventional Butler−Volmer formulation of electrode kinetics[36] which predicts a linear increase in *k* for all overpotentials. The solid lines of Figure 4 illustrate the best fits obtained from the nonadiabatic tunneling model where k° is 4.0×10^4, 1.8×10^4, and 3×10^3 s^{-1} for platinum, gold, and carbon, respectively, and λ is constant at 26 kJ mol^{-1}. These values agree with those found on the basis of fitting the scan rate dependent cyclic voltammograms to within 5%. Consistent with this low reorganization energy, the heterogeneous electron-transfer rate constant becomes independent of the electrical driving force for $\eta > 0.35$ V. Table 2 contains the standard heterogeneous electron-transfer rate constants, k°, obtained by extrapolating the potential dependent rate constants to zero overpotential. These data confirm that k° depends on the nature of the electrode material. It is important to consider the influence of double layer effects on k° which occur when the potential at the plane of electron transfer, ϕ_{PET}, is not equal to the potential in solution. For the monolayers considered here, double layer effects do not appear to be important for the following reasons. First, k° increases by less than 5% on going from 0.1 to 1.0 M supporting electrolyte. If double layer effects were significant, then the compression of the double layer caused by increasing the electrolyte concentration would alter ϕ_{PET} thus changing the apparent heterogeneous electron-transfer rate constant.

Second, the monolayers appear to be solvated and the double layer most likely sets up *within* the monolayer rather than at the monolayer/solution interface. For example, the interfacial capacitance is independent of the bulk electrolyte concentration, C_B, for $C_B > 0.2$ M and a limiting value of 25 ± 5 μF cm^{-2} is observed in 1.0 M $NaClO_4$ at −0.1 V. This value is independent of the electrode material used. This limiting value of the interfacial capacitance is considerably larger than that associated with a solvent-free monolayer.[37] This observation suggests that the electrochemical double layer sets up at the electrode/monolayer interface rather than at the monolayer/solution interface.

(36) Bard, A. J.; Faulkner, L. R. *Electrochemical Methods: Fundamentals and Applications*; Wiley: New York, 1980.

(37) Porter, M. D.; Bright, T. B.; Allara, D. L.; Chidsey, C. E. D. *J. Am. Chem. Soc.* **1987**, *109*, 3559.

Table 2. Standard Heterogeneous Electron-Transfer Rate Constants, $k°$, Activation Enthalpies, $\Delta H^{\ddagger}$, Reaction Entropies, $\Delta S_{RC}°$, Free Energies of Activation, $\Delta G^{\ddagger}$, and Preexponential Factors for the Metal-Based Redox Reaction within $[Os(OMe\text{-}bpy)_2(p3p)Cl]^{+/2+}$ Monolayers on Different Electrode Materials[a]

	$10^{-4}k^o/s^{-1}$	$\Delta H^{\ddagger}$/kJ mol^{-1}	$\Delta S^{\ddagger}$/J mol^{-1} K^{-1}	$\Delta G^{\ddagger}$/kJ mol^{-1}	$10^{-5}\upsilon_{el}/s^{-1}$ [b]	H_{AB}/J mol^{-1}
platinum	4.0 ± 0.2	11.3 ± 0.7	28 ± 4.5	7.3 ± 0.5	7.6 ± 1.7	0.47 ± 0.06
mercury	3.1 ± 0.3	10.6 ± 1.1	26 ± 5	6.9 ± 1.2	5.0 ± 3.1	0.38 ± 0.13
gold	1.8 ± 0.2	11.2 ± 0.5	32 ± 3	6.6 ± 0.3	2.6 ± 0.3	0.27 ± 0.02
silver	1.3 ± 0.2	11.2 ± 0.6	30 ± 4	6.9 ± 0.3	2.1 ± 0.3	0.24 ± 0.02
carbon	0.3 ± 0.03	11.1 ± 0.5	30 ± 4	6.8 ± 0.4	0.5 ± 0.08	0.12 ± 0.01

[a] Standard deviations are for at least three individual monolayers. Supporting electrolyte is aqueous 1.0 M $NaClO_4$. [b] Preexponential factor extracted from the standard heterogeneous electron-transfer rate constant using $\Delta G^{\ddagger}$.

Third, the potentials of zero charge (PZC) becomes more positive in the order Hg < Au < Pt. In the presence of double layer effects, one would anticipate that these PZCs would lead to $k°$s in the sequence Hg > Au > Pt. Table 2 clearly demonstrates that this is not the case for these monolayers.

As discussed above, caution must be exercised to ensure that apparent differences in $k°$ are not caused by variations in the free energy of activation, rather than by density of states. Therefore, we have probed the temperature dependence of k in order to extract enthalpies of activation.

Temperature Dependence of *k*. The activation enthalpy extracted from an Arrhenius plot of ln k vs T^{-1} measured at a constant potential has been termed "ideal",[31] and it is labeled here as $\Delta H_I^{\ddagger}$. For a reduction or cathodic reaction, this electrochemical activation enthalpy can be separated into a "chemical" activation enthalpy term, $\Delta H^{\ddagger}$, and a contribution from the "electrical" driving force, $\alpha_c F\phi_m$, where ϕ_m is the Galvani potential which corresponds to the formal potential of the reaction under consideration at a given temperature, according to eq 8.

$$\Delta H_{I,c}^{\ddagger} = -R\frac{\partial \ln k}{\partial(T^{-1})}|\phi_m = \Delta H^{\ddagger} - \alpha_c F\phi_m \qquad (8)$$

The temperature dependence of the heterogeneous electron-transfer rate has been investigated using temperature-resolved chronoamperometry over the range −5 to 40 °C. An overpotential of 50 mV, as determined at 298 K, was used throughout these experiments, and the resulting current−time transients were similar to those illustrated in Figure 2. The corresponding semilog plots were linear over approximately 1.5 lifetimes, and the heterogeneous electron-transfer rate was evaluated from the slopes. In a typical set of experiments, the temperature was systematically varied over a range and then returned to the initial temperature. The same slope, $-k$, and intercept, ln(kQ), were observed within experimental error for the initial and final transients. This consistency indicates that cycling the temperature does not change the heterogeneous kinetics or the quantity of material immobilized on the electrode surface. The heterogeneous electron-transfer rate increases with increasing temperature as anticipated for a thermally activated process. As illustrated in Figure 5, Arrhenius plots of ln k vs T^{-1} are linear ($R^2 > 0.995$) over the temperature range −5 to 40 °C. The slopes observed for the individual electrode materials are similar indicating that the activation enthalpy is independent of the identity of the electrode material. Table 2 contains the activation enthalpies, $\Delta H^{\ddagger}$, obtained from the slopes of these plots after using a transfer coefficient of 0.5 to correct for the electrical driving force (50 mV) according to eq 8. These data indicate that the average $\Delta H^{\ddagger}$ for all of the electrodes investigated is 11.1 ± 0.5 kJ mol^{-1}.

A deficiency in the foregoing analysis is that it fails to take account of the temperature dependence of the density of acceptor states within the electrode. In the Gosavi and Marcus model, this factor appears in the electronic coupling matrix element. Using an approach similar to that taken by Smalley and coworkers,[38] it may be possible to take into account the temperature dependence of both donor/acceptor states *and* the electrode density of states by using a plot of ln[$k°/T^{3/2}$] vs T^{-1} to determine the activation enthalpy. As illustrated in Figure 5, plots of [$k°/T^{3/2}$] vs T^{-1} are linear for each of the electrode materials investigated. Moreover, the slopes for the different electrode materials are identical to within experimental error indicating, as discussed above, that the activation enthalpy is independent of the electrode material. The slopes of these plots yield activation enthalpies that are approximately 30% smaller than those found using the conventional Arrhenius analysis.

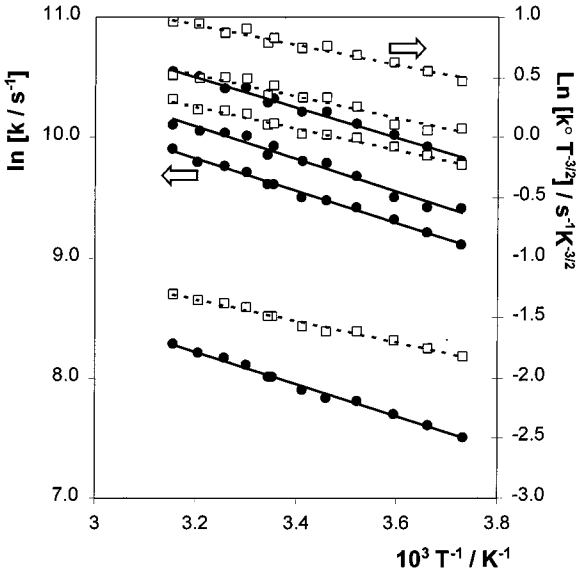

Figure 5. Temperature dependence of the heterogeneous electron-transfer rate constant for $[Os(OMe\text{-}bpy)_2(p3p)Cl]^+$ monolayers on temperature. The overpotential is 50 mV. From top to bottom, the electrodes are mercury, gold, silver, and carbon. The supporting electrolyte is aqueous 1.0 M $NaClO_4$. Filled circles and open squares and denote y-axes of ln(k) and ln[$k/T^{3/2}$], respectively. The error on measurements using three independent monolayers is comparable to the size of the symbol.

To use experimental enthalpies of activation to calculate free energies of activation it is necessary to determine the activation entropy. Comparing these values with the value of $\Delta G^{\ddagger}$ provided by fitting the high scan rate voltammetric data is an important test of consistency between these two independent approaches.

Reaction Entropies. The reaction entropy, $\Delta S_{rc}°$, quantifies the difference in entropy between the reduced and oxidized forms of the redox couple. The reaction entropy has been determined using a nonisothermal cell by measuring the

(38) Smalley, J. F.; Feldberg, S. W.; Chidsey, C. E. D.; Linford, M. R.; Newton, M. D.; Liu, Y.-P. *J. Phys. Chem.* **1995**, *99*, 13141.

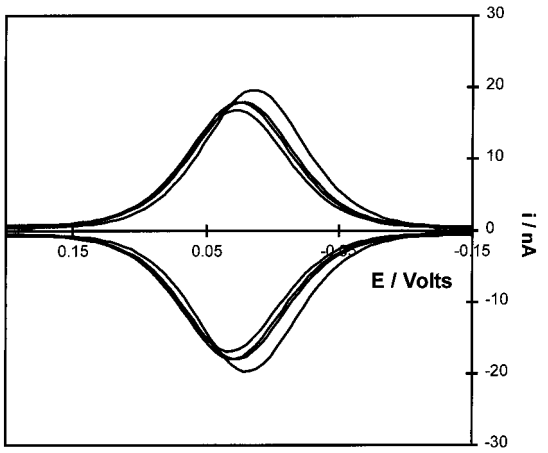

Figure 6. Temperature-dependent voltammetric response for an $[Os(OMe\text{-}bpy)_2(p3p)Cl]^+$ monolayer adsorbed on a 25 μm platinum microelectrode. From right to left the temperatures are −3, 5, 25, and 42 °C. The supporting electrolyte is aqueous 1.0 M $NaClO_4$.

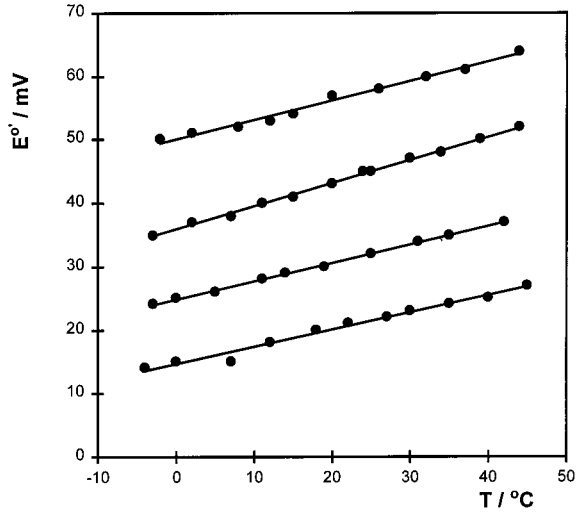

Figure 7. Effect of electrode material on the temperature dependence of the formal potential for the $Os^{2+/3+}$ redox reaction within $[Os(OMe\text{-}bpy)_2(p3p)Cl]^{+/2+}$ monolayers. From top to bottom, the electrodes are carbon, copper, platinum, and mercury. The formal potentials are reproducible to within 5 mV for independent monolayers.

temperature dependence of the $Os^{2+/3+}$ formal potential for monolayers on each of the electrode materials. As discussed by Weaver and co-workers,[14] the temperature dependence of the formal potential can be expressed as

$$\Delta S_{rc^\circ} = F(\partial E^{\circ\prime}/\partial T) \tag{9}$$

Figure 6 shows representative temperature-dependent cyclic voltammograms for the metal-based oxidation within $[Os(OMe\text{-}bpy)_2(p3p)Cl]^{+/2+}$ monolayers on a platinum microelectrode. For monolayers assembled on each of the electrode materials investigated, the formal potential shifts in a positive potential direction with increasing temperature. This observation indicates positive reaction entropies and a higher degree of local ordering in the oxidized than in the reduced state. As shown in Figure 7, plots of $E^{\circ\prime}$ vs T are linear over the temperature range −5 to 40 °C, and reaction entropies have been calculated from the slopes according to eq 9. Experimentally, the magnitude of ΔS_{rc}° is independent of the identity of the electrode material with a value of 29.6 ± 2.4 J mol^{-1} K^{-1}. Given that the reaction entropy is sensitive to the local dielectric constant within the monolayer, this result indicates that the microenvironments within the monolayers are all similar. Moreover, the entropy observed is similar to that found for monolayers constructed using related bipyridyl complexes[17,18] suggesting that changes in the structure, e.g., incorporation of methoxy moieties, do not significantly change the extent of solvent ordering within the monolayers.

The entropy of the transition state is assumed to lie between that of the reduced and oxidized forms, and the cathodic free energy of activation is given by

$$\Delta G_c^{\ddagger} = \Delta H_c^{\ddagger} - T\alpha_c \Delta S_{rc}^{\ o} \tag{10}$$

where α_C is the cathodic transfer coefficient. Table 2 shows that the free energy of activation is approximately independent of the type electrode material on which the monolayer is assembled. Taken together, these enthalpy, entropy, and free energy data represent a powerful argument that the activation parameters for the $Os^{2+/3+}$ redox reaction within $[Os(OMe\text{-}bpy)_2(p3p)Cl]^{+/2+}$ are indistinguishable for platinum, mercury, gold, silver, and carbon electrodes.

Preexponential Factor. Table 2 contains values for the electron hopping frequency υ_{el} that have been determined using eq 1 and the experimental values of $\Delta G_c^{\ddagger}$ and k°. Consistent with the modeling of the voltammetric response illustrated in Figure 2, irrespective of the identity of the electrode material, these prefactors are approximately 6 orders of magnitude smaller than those expected for an adiabatic electron-transfer reaction.[39] Table 2 also suggests that υ_{el} is sensitive to the identity of the electrode material. However, in the calculation of υ_{el}, the exponential relationship of eq 1 tends to amplify the small variations observed in $\Delta G^{\ddagger}$. Nevertheless, the large difference in electron hopping frequencies between platinum and carbon might be expected given the known sensitivity of heterogeneous electron transfer to the density of edge-planes in carbon electrodes.[40,41] More significant perhaps, are the differences observed between Pt and Au where the $\Delta G^{\ddagger}$ values are indistinguishable.

The density of states, ρ_F, of platinum is approximately 7.5 times that of gold, which, according to traditional theory, is expected to cause a proportional increase in υ_{el}. However, the Marcus and Gosavi[5] model highlights the importance of considering the identity of the orbitals that are responsible for increasing ρ_F. For example, the d-orbitals found in platinum that lead to an increased density of states are expected to couple less efficiently than the dominant sp-states of gold. Thus, the Marcus model predicts a ratio of $k^\circ_{Pt}/k^\circ_{Au}$ of 1.8. Superficially, our experimental value of 2.2 ± 0.4 compares favorably with this theoretical prediction. However, it is important to use the experimental data to probe the theoretical prediction that the electronic coupling per state is lower for platinum than for gold.

Electronic interaction of the redox orbitals and the metallic states causes splitting between the product and reactant hypersurfaces which is quantified by H_{AB}, the matrix coupling element. The Landau−Zener treatment[42] of a nonadiabatic reaction yields

$$\upsilon_{el} = (2H_{AB}^{\ 2}/h)(\pi^3/\lambda RT)^{1/2} \tag{11}$$

where h is Planck's constant. The matrix coupling element has been determined for each of the electrode materials, and the

(39) Weaver, M. J. *Chem. Rev.* **1992**, *92*, 463.
(40) Ray, K. G.; McCreery, R. L. *J. Electroanal. Chem.* **1999**, *469*, 150.
(41) McCreery, R. L.; Cline, K. K.; McDermott, C. A.; McDermott, M. T. *Colloids Surf. A* **1994**, *93*, 211.
(42) Brunschwig, B. S.; Sutin, N. *Coord. Chem. Rev.* **1999**, *187*, 233.

results are presented in Table 2. The fact that H_{AB} is less than 1 kJ mol^{-1} confirms that the system is charge localized and nonadiabatic.[42] These monolayers provide a significant opportunity to compare the extent of electronic communication across the p3p bridge when bound to a metal electrode as opposed to being coupled to a molecular species, e.g., within a dimeric metal complex. For example, Taube and co-workers[43] have used intervalence charge-transfer intensities to probe the extent of electronic coupling across 4,4′-dipyridyl type bridges in which the pyridine rings are separated by a number of methylene spacer groups. Asymmetric dimers linked by related bridging ligands have also been investigated.[44] Dimeric complexes of this type exhibit H_{AB} values between approximately 2 and 10 kJ mol^{-1} and are categorized as class II compounds according to the Robin−Day system.[45] Significantly, the H_{AB} values for the monolayers investigated here are approximately 4 orders of magnitude smaller than those found in dimers. This behavior indicates that the metal center interacts much more weakly with the electrode surface than with another metal center. However, the observation that H_{AB} is approximately 1.8 times larger for platinum than for gold suggests that the higher density of states on platinum relative to gold is not offset by a lower electronic coupling per state as predicted by theory. In this sense, models that assume the heterogeneous electron-transfer rate is proportional to the density of states modulated by the square of the electronic coupling may be incomplete. It is perhaps important to note that probing metal-to-metal charge transfer interactions within mixed valence complexes is an excited-state process as opposed to the thermally activated ground-state process investigated here. Future experiments will probe this issue by measuring rate constants for oxidation of electronically excited monolayers generated using pulsed laser methods.[46]

(43) Taube, H. In *Tunneling in Biological Systems*; Chance, B., Ed.; Academic Press: New York, 1979; p 173.
(44) Fagalde, F.; Katz, N. E. *Polyhedron* **1995**, *14*, 1213.
(45) Brunschwig, B. S.; Creutz, C.; Sutin, N. *Coord. Chem. Rev.* **1998**, *177*, 61.
(46) Forster, R. J.; Keyes, T. E. *J. Phys. Chem. B* **1998**, *102*, 10004.

Conclusions

Adsorbed monolayers of $[Os(OMe\text{-}bpy)_2(p3p)Cl]^+$ have been formed on platinum, mercury, gold, silver, and carbon microelectrodes, where OMe-bpy is 4,4′-2,2′-dimethoxybipyridyl and p3p is 1,4-trimethylenedipyridine. They exhibit nearly ideal electrochemical responses as the potential, temperature, and experimental time scale are varied over a wide range. These monolayers have been used to probe the effect of changing the density of electronic states within the electrode on the heterogeneous electron-transfer rate. Both high scan rate cyclic voltammetry as well as temperature-resolved chronoamperometry and cyclic voltammetry reveal that the free energy of activation is consistent with that expected for a simple outer sphere reaction. The experimental preexponential factors are consistent with those expected for a nonadiabatic reaction in which there is weak electronic coupling between the delocalized metallic states on the electrode and the localized redox states of the osmium complex. The ratio of the prefactors for platinum and gold is 2.9 ± 0.7 compared with a ratio of 7.5 for the density of states. Therefore, our experimental data indicate that the nonadiabatic rate of heterogeneous electron transfer does not depend simply on the density of states within the electrode.

Acknowledgment. The expert advice of Dr. Chris Taylor and Prof. Adam Heller of the University of Texas at Austin on the synthesis of $[Os(OMe\text{-}bpy)_2Cl_2]$ is deeply appreciated. The assistance of Professor Marcus and Dr. Gosavi by providing an advance copy of ref 5 is gratefully acknowledged. We thank Professor Finklea for providing related experimental data on alkanethiol monolayers deposited on gold, silver, and platinum electrodes. We appreciate the ongoing financial support from Enterprise Ireland, the Irish Science and Technology Agency, under Basic Research Grant SC/99/132. The generous loan of potassium hexachloroosmate(IV) by Johnson Matthey under the loan scheme is deeply appreciated. We appreciate the reviewer's suggestion for the alternative analysis of the temperature-dependent rate constant data.

JA002616U